HHS Public Access

Author manuscript

Cancer Res. Author manuscript; available in PMC 2021 September 22.

Published in final edited form as:

Cancer Res. 2021 February 15; 81(4): 885–897. doi:10.1158/0008-5472.CAN-19-3219.

Cancer-induced muscle wasting requires p38β MAPK-mediated activation of p300

Thomas K. Sin[1,♣], **Guohua Zhang**[1,♣], **Zicheng Zhang**[1], **James Z. Zhu**[1], **Yan Zuo**[1], **Jeffrey A. Frost**[1], **Min Li**[1,2,3,4], **Yi-Ping Li**[1,*]

[1]Department of Integrative Biology and Pharmacology, The University of Texas Health Science Center at Houston, 6431 Fannin Street, Houston, TX 77030, USA

[2]The Vivian L. Smith Department of Neurosurgery, The University of Texas Health Science Center at Houston, Houston, TX 77030, USA

[3]Department of Medicine, The University of Oklahoma Health Sciences Center, Oklahoma City, OK 73104, USA

[4]Department of Surgery, The University of Oklahoma Health Sciences Center, Oklahoma City, OK 73104, USA

Abstract

Cancer-associated cachexia, characterized by muscle wasting, is a lethal metabolic syndrome without defined etiology or established treatment. We previously found that p300 mediates cancer-induced muscle wasting by activating C/EBPβ, which then upregulates key catabolic genes. However, the signaling mechanism that activates p300 in response to cancer is unknown. Here we show that upon cancer-induced activation of Toll-like receptor 4 (TLR4) in skeletal muscle, p38β MAPK phosphorylates Ser-12 on p300 to stimulate C/EBPβ acetylation, which is necessary and sufficient to cause muscle wasting. Thus, p38β MAPK is a central mediator and therapeutic target of cancer-induced muscle wasting. In addition, nilotinib, an FDA-approved kinase inhibitor that preferentially binds p38β MAPK, inhibited p300 activation 20-fold more potently than the p38α/β MAPK inhibitor SB202190 and abrogated cancer cell-induced muscle protein loss in C2C12 myotubes without suppressing p38α MAPK-dependent myogenesis. Systemic administration of nilotinib at a low dose (0.5 mg/kg/day, IP) in tumor-bearing mice not only alleviated muscle wasting but also prolonged survival. Therefore, nilotinib appears to be a promising treatment for human cancer cachexia due to its selective inhibition of p38β MAPK.

Keywords

Cachexia; lung cancer; pancreatic cancer; experimental therapy; nilotinib

*To whom correspondence should be addressed: Yi-Ping Li, Department of Integrative Biology and Pharmacology, The University of Texas Health Science Center at Houston, 6431 Fannin Street, Houston, Texas 77030, USA. Tel: (713) 500-6498, Fax: (713) 500-0689, yi-ping.li@uth.tmc.edu.

♣These authors contributed equally.

Author contributions:

Y.-P.L. and G. Z. designed the experiments, T.K.S., G.Z., Z.Z., J.Z.Z. performed the experiments and interpreted the results, Z.Y. and J.A.F. helped with methodology, T.K.S., G.Z., J.A.F., M.L. and Y.-P.L. wrote, discussed and edited the paper.

Introduction

Cancer has been increasingly recognized as a systemic disease that causes disorders in multiple organs that are not resided by cancer *per se*. Cachexia is a metabolic syndrome seen in approximately 60% of cancer patients (1). Cachexia is defined as a multifactorial syndrome characterized by an ongoing loss of skeletal muscle mass (with or without loss of fat mass) that cannot be fully reversed by conventional nutritional support and leads to progressive functional impairment. Clinical manifestations of cachexia include weight loss, inflammation, insulin resistance, and increased muscle protein breakdown (2). Not only does cachexia increase patients' morbidity and mortality through systemic wasting, but it also decreases the efficacy while increasing the toxicity of chemotherapy (3). Consequently, cachexia is the direct cause of ~1/3 of cancer-related deaths (4). Thus, cachexia is a major determinant for survival of cancer patients. Adequate management of cachexia would preserve muscle and body mass, improve patient physical condition and quality of life to withstand cancer treatment, and could enhance cancer treatment outcomes and overall survival. However, there is no established treatment for cancer cachexia due to the poor understanding of its etiology. In 2020, 1,806,590 new cancer cases and 606,520 cancer deaths are projected in the United States (5), so the unmet medical need for treating cancer cachexia is substantial. Thus, we seek to decipher the underlying etiology and thereby to identify therapeutic strategies for cancer cachexia.

Cancer provokes muscle wasting through complex signaling mechanisms that may be targeted for therapeutic purposes. We have previously showed that cachexia-inducing cancers release high levels of Hsp70 and Hsp90 through extracellular vesicles, which activate TLR4 on skeletal muscle cells to induce muscle catabolism directly, and activate TLR4 systemically to increase circulating inflammatory cytokines such as TNFα and IL-6, which also that promote muscle catabolism (6,7). We have also reported that activation of the β isoform of p38 MAPK is required for cancer-induced muscle protein loss due to its activation of C/EBPβ-DNA binding. This occurred through p38 MAPK-dependent phosphorylation of C/EBPβ on Thr-188, leading to transactivation of key genes in the ubiquitin-proteasome (*atrogin1/MAFbx* and *UBR2*) and the autophagy-lysosome (*LC3b* and *Gabarapl1*) pathways (8–11). In addition, p38β MAPK mediates cancer-induced activation of ULK1 by phosphorylating its Ser-555 residue, a critical step for autophagosome formation (11). Furthermore, we have demonstrated most recently that the acetyltransferase p300 is also required for cancer-induced muscle wasting due to its activation of C/EBPβ through site-specific acetylation on Lys-39, in spite of intact phosphorylation of C/EBPβ on Thr-188 mediated by p38β MAPK (12). However, the mechanism through which p300 is activated by cancer is unknown. In the present study, we sought to identify the upstream signal that activates p300 during cancer-induced muscle wasting, and to evaluate whether this pathway can be targeted pharmacologically for intervention in cancer cachexia.

We show here that cancer induces p300 activation through TLR4-mediated activation of p38β MAPK. Specifically, p38β MAPK phosphorylates Ser-12 on p300 to stimulate its acetyltransferase activity, which in turn activates C/EBPβ through Lys-39 acetylation. These findings indicate that p38β MAPK is indispensable for cancer-induced muscle wasting through the activation of the p300 – C/EBPβ signaling pathway, and suggest that

inhibiting p38β MAPK could be an effective therapeutic strategy for intervening cancer-induced muscle wasting. Unfortunately, p38β MAPK-specific small molecule inhibitors are not available. Therefore, we tested the efficacy of the protein kinase inhibitor nilotinib (Tasigna®, Novartis Pharmaceuticals), approved by FDA for chronic myelogenous leukemia (CML), at inhibiting p38β MAPK activation of p300 based on the fact that nilotinib has a significantly higher binding affinity for p38β MAPK than p38α MAPK or its originally intended target BCR-ABL (13). We found that nilotinib inhibits cancer-induced activation of p300 and C/EBPβ in skeletal muscle cells that is mediated by p38β MAPK at a concentration 20-fold lower than the p38α/β MAPK dual inhibitor SB202190, without affecting myogenic differentiation that is mediated by p38α MAPK. Systemic administration of nilotinib to diverse types of tumor-bearing mice at a dose that is at least 30 times lower than used for treatment of mouse models of leukemia alleviated muscle wasting and prolonged survival. These data suggest that cancer-induced muscle wasting can be effectively treated by repurposing nilotinib to inhibit p38β MAPK.

MATERIALS AND METHODS

Cell cultures

Murine C2C12 myoblasts (American Type Culture Collection, ATCC) and human skeletal myoblasts (GIBCO®) were grown in growth medium (DMEM supplemented with 10% fetal bovine serum) at 37°C under 5% CO_2. Myoblast differentiation was induced at 85% confluence with differentiation medium (DMEM supplemented with 4% heat-inactivated horse serum in) for 96 hrs. Conditioned medium from 48-hour cultures of Lewis lung carcinoma (LLC) cells (National Cancer Institute, Frederick, MD), H1299 human lung carcinoma cells (ATCC) or KPC cells (a gift from Dr. Elizabeth Jaffee of Johns Hopkins University) (14) were collected and centrifuged (1000 x g, 5 min). Conditioned medium of non-tumorigenic NL20 cells (human lung epithelial cells, ATCC) was used as control. The supernatant was used to treat myotubes (25% final volume in fresh medium) when indicated, and replaced every 24 h. When indicated, myotubes were pre-treated with nilotinib (CDS023093, Sigma, St. Louis, MO) for 30 mins at doses ranging from 10 nM to 10 μM. All cell lines were tested negative for mycoplasma contamination. Cell culture-based experiments were replicated independently for 3 times. Cell lines were free of mycoplasma as determined using MycoAlert™ PLUS Mycoplasma Detection Kit (Lonza, Basel, Switzerland) on October 16, 2018. C2C12 myoblasts were passed under 10 passages from the stock. Cancer cell lines were passed no more than 4 times from the stock.

Transfection of siRNA and plasmids in C2C12 myotubes

At 60% confluence, C2C12 myoblasts were transfected with siRNA targeting p38α MAPK (SASI_Mm01_00020743), p38β MAPK (SASI_Mm01_00044863) or ABL1 (SASI_Rn02_00322591) from Sigma Aldrich or scramble control siRNA (Ambion, Austin, TX). For overexpression studies, myoblasts were transfected with plasmids encoding p300 phosphorylation-defective mutants (p300-S12A or p300-S89A) (15), p300 phosphomimic mutant (p300-S12D) or constitutive active mutants of p38α or p38β MAPK (16). All transfections were performed with jetPRIME reagent (Polyplus-transfection Inc., Illkirch, France) according to the manufacturer's protocol. Growth medium was replaced with

differentiating medium 24 hours after transfection to induce differentiation as described earlier.

Animal use

Experimental protocols were pre-approved by the institutional Animal Welfare Committee at the University of Texas Health Science Center at Houston. Experimental mice were group-housed, kept on 12:12 h light-dark cycle with access to standard rodent chow and water ad libitum. LLC cells (1×10^6 in 100 μl) were injected subcutaneously into the flanks of 8-week-old male C57BL/6 mice, $TLR4^{-/-}$ mice in the C57BL/6 background (17), or p38β MAPK muscle-specific knockout and p38β MAPK-floxed mice in the C57BL/6 background (18). Nilotinib treatment was initiated seven days after LLC cell implantation when palpable tumor was detected through the intraperitoneal route (0.5 mg/kg/day prepared in 50% DMSO in PBS). DMSO was injected accordingly as vehicle control. Orthotopic implantation of KPC cells was performed based on the procedures by Zhu et al. (19). Briefly, a longitudinal incision was made to open the abdominal cavity for pancreas exposure. Then, 2 X 10^6 KPC cells (stably transfected with a plasmid encoding luciferase) suspended in 20 μl PBS were injected to the tail of pancreas. Nilotinib (0.5 mg/kg/day) was administered intraperitoneally from five days after tumor implantation until predetermined end point was reached. Plasmid encoding the p300-S12A mutant was transfected into tibialis anterior (TA) muscle by electroporation on day 7 and day 14 following tumor cell implantation as described previously (12). The contralateral TA was transfected with an empty vector as control. In separate experiments, p300–12D was overexpressed in TA muscle of tumor-free mice. Development of cachexia was monitored by body weight and forelimb grip strength test, and usually took place within 21 days after implantation of either types of tumor cells.

Plasmid construction

Plasmid encoding a phosphomimic mutant of p300, p300-S12D, was constructed by using the Q5 Site-Directed Mutagenesis Kit (E0554S from New England BioLabs, Ipswich, MA) with wild-type mouse p300 as template. Forward and reverse primers were designed by NEB online design software (F-cgggccgcctgatgccaagcggc, R-ggttccaccacattctcggc). Manufacturer's protocol was followed with annealing temperature at 71°C. The sequencing primer (ccaatctgctgtccagaattctg) was used for verification.

Western blotting

All procedures were adhered to our previous publication (12). The following primary antibodies were used: anti-p300 (1:500, sc584, Santa Cruz), anti-C/EBPβ (1:1000, MA1–827, Thermo Fisher), anti-pT188-C/EBPβ (1:1000, 3084, Cell Signaling Technology), anti-TLR4 (1:500, sc16240, Santa Cruz), anti-p38α MAPK (1:500, sc271120, Santa Cruz), anti-p38β MAPK (1:500, 2339, Cell Signaling Technology), anti-p38 MAPK (1:1000, 9212, Cell Signaling Technology), anti-p-p38 MAPK (1:1000, 4511, Cell Signaling Technology), anti-MAFbx (1:1000, AP2041, ECM Bioscience), anti-UBR2 (1:500, NBP1–45243, Novus Biologicals), anti-LC3 (1:2000, NB100–2220, Novus Biologicals) and anti-MHC (1:1000, MAB4470, R&D Systems). Antibody against acetylated Lys-39 of C/EBPβ (1:2000) was generated as previously described (12). Antibody against phosphorylated Ser-12 of p300

(1:1500) were generated by Pocono Rabbit Farm & Laboratory (Canadensis, PA) from rabbit using the peptide PGPPS(P)AKRPKLSSPAC. The specificity of the antibody was validated using mutated p300 with point mutantions (Figure 1A). Data were normalized to α-Tubulin (Development Studies Hybridoma Bank at the University of Iowa, Iowa City, IA).

Fluorescence microscopy and histology study

C2C12 myotubes were stained with anti-MHC antibody (1:1000, MAB4470, R&D Systems) and anti-mouse Alexa Fluor® Plus 488 secondary antibody (1:200, A32723, ThermoFisher), and examined using a Zeiss Axioskop 40 microscope and a Zeiss Axiocam MRM camera system controlled by Axiovision Release 4.6 imaging software. Acquired images were edited using the Photoshop software. Myotube diameter was measured in MHC-stained myotubes as previously described (12). Cross-sectional area of H&E-stained muscle sections was quantified by using the ImageJ software (NIH). Approximately 100 myofibers from each of 5 random views were quantified.

Parafilm-embedded tumor sections were first baked overnight prior to hydration in the chronological order of xylene and decreasing concentration of ethanol (100% > 95% > 70%). Antigen retrieval was performed by incubating the slides in 10 mM sodium citrate (pH 6) using a pressure cooker for 15 mins. After cooling, endogenous peroxidase was quenched by 3% H2O2 for 30 mins. After 5 washes in PBS, the sections were blocked in goat serum for 30 minutes (S-1012, Vectastain, CA) followed by overnight incubation with Ki67 antibody (12202, 1:200, Cell Signaling) overnight at 4°C. The slides were washed and incubated with anti-rabbit secondary antibody (1:200) at room temperature for 1 h. After 5 washes, ABC staining was performed according to the manufacturer's instructions (PK-4000, Vectastain). The sections were then stained with DAB reagents (TA-125-QHDX, Thermo Fisher, UK) for 5 minutes and counter-stained with haemotoxylin (MHS80, Sigma-Aldrich). Dehydration was then performed in the reverse order of hydration before mounting.

Immunoprecipitation

Immunoprecipitation of p38 MAPK from myotube lysate (1 mg of protein) was performed using an anti-p38 MAPK antibody (1:100; CS9212, Cell Signaling) as described previously (8).

Statistical analyses

Statistical analyses were conducted using the SPSS 22.0 software package (IBM, Chicago, IL). Data distributions were confirmed by the normality test. All data were expressed as means ± standard deviation (SD). Comparisons were made by one-way ANOVA followed by Tukey post-hoc test, Paired t-test, Chi-Square test and two-way ANOVA as appropriate. Statistical significance was accepted at $p < 0.05$.

Results

Muscle wasting induced by diverse types of cancer requires site-specific phosphorylation of p300 on Ser-12 to activate C/EBPβ

Based on our previous observation that p300 activates C/EBPβ through acetylating its Lys-39 residue in response to Lewis lung carcinoma cell-conditioned medium (LCM) treatment in C2C12 myotubes within an hour (12), we reasoned that the underlying regulatory mechanism of this reaction involved posttranslational modification of p300. It was previously shown that p300 has at least two N-terminal phosphorylation sites, Ser-12 and Ser-89; the former is unique and its phosphorylation is critical to the substrate-binding activity of p300 (15). Therefore, we tested whether cancer activates p300 in skeletal muscle cells through the phosphorylation of its Ser-12 residue. To do so we generated a polyclonal antibody that specifically recognizes p300 phosphorylated on Ser-12 (p-Ser12-p300). Plasmids encoding phosphorylation-defective mutants of p300 with serine-to-alanine mutations at Ser-12 (p300-S12A) or Ser-89 (p300-S89A) (15) were transfected into C2C12 myoblasts. After differentiation, myotubes were treated with LCM and p300 activation was analyzed by Western blotting using the antibody against p-Ser12-p300. As shown in Figure 1A, LCM treatment robustly increased Ser-12 phosphorylation of p300 as well as Lys-39 acetylation of C/EBPβ. The latter is mediated by activated p300 (12). Overexpression of p300-S12A, but not p300-S89A, abrogated Ser-12 phosphorylation of p300 and subsequent Lys-39 acetylation of C/EBPβ, suggesting that LCM induces activation of p300 to acetylate C/EBPβ in myotubes through the phosphorylation of its Ser-12 residue. These data also demonstrate the specificity of the custom-made antibody against p-Ser12-p300. To assess whether p300 phosphorylation on Ser-12 is required for LLC-induced muscle mass loss *in vivo*, the p300-S12A plasmid was overexpressed in the tibialis anterior (TA) of mice bearing an LLC tumor and verified by Western blotting (Figure 1B). While vector-transfected TA (control) lost approximately 20% of its weight, the contralateral TA transfected with the p300-S12A plasmid was spared from weight loss (Figure 1B). Histological analyses of cross sections of the TA samples verified that the p300-S12A mutant protected muscle from LLC-induced loss in muscle mass as measured by myofibril cross-sectional area (Figure 1C).

To assess whether other types of cancer induces muscle wasting by activating p300 phosphorylation on Ser-12, p300-S12A was overexpressed in the TA of C57BL/6 mice orthotopically implanted (19) with syngeneic KPC cells (14), a mouse pancreatic ductal adenocarcinoma (PDAC) cell line derived from the original KPC mouse (20). Overexpressed p300-S12A attenuated loss of muscle weight (Figure 1D) and myofiber mass as measured by cross-sectional area (Figure 1E) in KPC tumor-bearing mice similar to LLC tumor-bearing mice. Furthermore, to determine whether p300 phosphorylation on Ser-12 is sufficient to cause muscle wasting, we constructed and overexpressed a phosphomimic mutant of p300 (p300-S12D) in the TA of mice without tumors. This mutant recapitulated tumor-induced loss of TA weight (Figure 1F) and myofiber cross-sectional area (Figure 1G), indicating that phosphorylation of p300 on Ser-12 alone is sufficient to cause muscle wasting. These results allow us to conclude that cancer induces muscle wasting through site-specific

phosphorylation of p300 on Ser-12 to activate the acetyltransferase activity of p300 that in turn activates C/EBPβ by acetylating its Lys-39 residue.

TLR4 mediates LLC-induced activation of p300

To decipher the signaling mechanism through which LLC induces p300 activation, we hypothesized that p300 is a downstream effector of TLR4 based on previous findings that TLR4 mediates muscle catabolism in response to LLC cell-released Hsp70 and Hsp90 (6,7). To test this, we knocked down TLR4 in C2C12 myotubes using a specific-siRNA and observed that LCM-induced p300 phosphorylation on Ser-12 and C/EBPβ acetylation on Lys-39 required TLR4 (Figure 2A). Then, by comparing wild type mice with $TLR4^{-/-}$ mice we verified *in vivo* that LLC tumor-induced activation of p300 in the TA muscle required TLR4 (Figure 2B). These findings are congruent with our previous report that $TLR4^{-/-}$ mice are resistant to LLC tumor-induced muscle wasting including loss of myofiber cross-sectional area (6). Thus, LLC tumor activates the acetyltransferase activity of p300 through TLR4 to induce muscle wasting.

p38β MAPK mediates p300 activation in muscle induced by diverse types of cancer cells

To identify the TLR4 effector that mediates Ser-12 phosphorylation of p300, we tested the role of p38β MAPK based on previous findings that it functions downstream of TLR4 in tumor-induced muscle wasting (11,21). Utilizing siRNA-mediated knockdown of p38α or p38β MAPK we observed that only p38β MAPK, but not p38α MAPK, was critical to LCM-induced p300 phosphorylation on Ser-12 and C/EBPβ acetylation on Lys-39 in myotubes (Figure 3A). Given that p38β MAPK-mediated muscle protein loss is also activated by human PDAC cell lines (AsPC-1 and BxPC-3) that are potent inducers of cachexia (22), we investigated whether p38β MAPK also activates p300 in response to pancreatic cancer by utilizing KPC cells. Similar to LCM, treatment of myotubes with conditioned medium from KPC cells (KCM) provoked a robust increase in Ser-12 phosphorylation of p300 as well as Lys-39 acetylation of C/EBPβ. In contrast, these increases were abrogated in p38β MAPK-deficient myotubes (Figure 3B). These data indicate that diverse types of cachexia-inducing cancer cells activate the acetyltransferase activity of p300 in a p38β MAPK-dependent manner. Conversely, over-expression in myotubes a constitutively active mutant of p38β MAPK (16), but not p38α MAPK, recapitulated the site-specific p300 phosphorylation and C/EBPβ acetylation seen in LCM/KCM-treated myotubes (Figure 3C). To investigate whether LCM stimulated an interaction between p38β MAPK and p300 we performed immunoprecipitation to pull down total p38 MAPK from myotube lysate. Indeed, p300 was co-precipitated with p38 MAPK at baseline, which was increased dramatically in response to LCM. By contrast, this elevation was abrogated in myotubes that are deficient in p38β MAPK, but not p38α MAPK (Figure 3D), indicating that LCM-activated p38β MAPK specifically interacts with p300, resulting in its phosphorylation on Ser-12. To verify whether p38β MAPK mediates the phosphorylation and activation of p300 *in vivo*, we found that in p38β MAPK muscle-specific knockout mice (p38β mKO) that are resistant to LLC-induced muscle wasting (11) LLC tumors failed to induce p300 phosphorylation on Ser-12 and C/EBPβ acetylation on Lys-39 in TA muscle (Figure 3E). These observations are consistent with our previous report that p38β MAPK muscle-specific knockout mice are resistant to LLC tumor-induced loss of muscle mass and

myofiber cross-sectional area (11). These data indicate that p38β MAPK is a key mediator of cancer-induced muscle wasting due to its activation of the p300 − C/EBPβ signaling pathway in response to TLR4 activation.

Nilotinib protects against LLC tumor-induced muscle wasting by selective inhibition of p38β MAPK

To assess the translatability of our preclinical findings into a potential clinical intervention of cancer cachexia, we searched for a pharmacological inhibitor of p38β MAPK suitable for human use. The p38 MAPK family has four members with distinctive functions, of which three are expressed in skeletal muscle (α, β and γ) (23). Existing p38 MAPK inhibitors are either p38α/β dual inhibitors or p38α-specific inhibitors, which are not suitable for intervening cancer cachexia due to the essential role of p38α MAPK in myogenic differentiation (24,25). Cancer cachexia compromises myogenic differentiation through TLR4-mediated activation of NF-κB (26,27), so inhibiting p38α MAPK would further impede the regeneration of cachectic muscle. In addition, p38α MAPK, but not p38β MAPK, is responsible for most of the known biological activities of p38 MAPK (28,29). Thus, it is necessary to have a protein kinase inhibitor that is selective for p38β MAPK in the intervention of cancer cachexia in humans. The small molecule BCR-ABL kinase inhibitor nilotinib is an FDA-approved therapy for chronic myelogenous leukemia (CML) and exhibits 3-fold higher binding affinity for p38β MAPK than for p38α MAPK (13), making it the only relatively p38β MAPK-selective inhibitor available for human use. Importantly, the very high binding affinity of nilotinib for p38β MAPK (Kd = 32 nM) is about twice of that for its originally intended target BCR-ABL (Kd = 56–62 nM) (13), suggesting that lower doses of nilotinib would be sufficient to inhibit p38β MAPK, and hence, fewer non-specific effects and lower toxicity can be expected. Therefore, we investigated the efficacy of nilotinib in blocking muscle wasting in cell culture and in mouse models of cancer cachexia.

A concentration-activity study in C2C12 myotubes revealed that nilotinib inhibited LCM-induced p300 phosphorylation on Ser-12 in a concentration-dependent manner. Notably, nilotinib totally abolished this reaction at 500 nM, which was about 20-fold more potent than SB202190, a p38α/β dual inhibitor that attenuates LLC tumor-induced muscle wasting in mice (8). Concordantly, C/EBPβ acetylation on Lys-39 was inhibited by nilotinib in a similar manner (Figure 4A). These results indicate that nilotinib is highly efficacious at inhibiting the activation of the acetyltransferase activity of p300 by LLC. Nilotinib inhibited LCM-induced upregulation of C/EBPβ-controlled E3 ligase UBR2 (10) in C2C12 myotubes in a similar concentration-dependent manner, confirming the inhibition of C/EBPβ-mediated catabolic signaling by nilotinib (Figure S1). To assess whether nilotinib inhibits myotube p38 MAPK activation by cancer in general, we observed that pretreating primary human myotubes with 500 nM of nilotinib abrogated p38 MAPK activation by conditioned medium of the human lung carcinoma cell line H1299, resulting in a blockade of p38β MAPK-mediated C/EBPβ phosphorylation on Thr-188 (9) and upregulation of E3 ligase UBR2 (10) (Figure S2). This result suggests that nilotinib inhibits human cancer-induced p38 MAPK activation and the ensuing catabolic response in human muscle cells. Similarly, C2C12 myotubes treated with 500 nM nilotinib were protected from LCM-induced loss of

myofibrillar protein myosin heavy chain (MHC) (Figure 4B) and myotube mass as measured by myotube diameters (Figure 4C). These effects were comparable to the effects of 10 μM of SB202190 reported previously (8), demonstrating the high efficacy of nilotinib in inhibiting p38β MAPK-mediated muscle protein degradation.

To examine whether the observed effect of nilotinib occurred via inhibition of ABL1, the ABL1 gene in C2C12 cells was knocked down with siRNA, considering that ABL2 knockdown would affect myoblast proliferation and fusion (30). ABL1 expression did not respond to LCM with or without Nilotinib treatment in ABL1-deficient myotubes (Figure S3A). LCM upregulated the mRNA of UBR2 (Figure S3B), atrogin1/MAFbx (Figure S3C) and LC3b (Figure S3D) as expected in both control myotubes and ABL1-deficient myotubes, and nilotinib treatment abolished this upregulation similarly in both types of myotubes (Figure S3). Thus, the anti-muscle protein degradation activity of nilotinib does not involve its inhibition of ABL1.

To assess the specificity of nilotinib for p38β MAPK, we analyzed the effect of nilotinib on myogenic differentiation, which requires p38α MAPK (24,25). C2C12 myoblasts were allowed to differentiate for 96 h in the presence of 500 nM of nilotinib or 10 μM of SB202190. SB202190 delayed the onset of myoblast differentiation as indicated by significantly lower expression of MHC at 24 and 48 h in comparison to control cells. In contrast, nilotinib did not inhibit MHC expression over the course of differentiation (Figure 4D). This result suggests that at 500 nM nilotinib selectively inhibited p38β MAPK without affecting p38α MAPK. Of note, 500 nM of nilotinib exerted maximum inhibition of p300 activation as shown in Figure 4A, which means that the therapeutic dose of nilotinib for cancer-induced muscle wasting would fall within its p38β MAPK-selective dose range.

To determine whether nilotinib ameliorates cancer-induced muscle wasting *in vivo,* nilotinib was administered intraperitoneally to LLC tumor-bearing mice at a dose of 0.5 mg/kg/day for 2 weeks, starting at day 7. Similar to its effects *in vitro*, nilotinib abrogated the phosphorylation of p300 on Ser-12 and subsequent Lys-39 acetylation of C/EBPβ, resulting in a blockade of upregulation of C/EBPβ-controlled E3 ligases UBR2 and atrogin1/MAFbx. Nilotinib treatment also blocked activation of autophagy measured by LC3-II levels. Consequently, loss of MHC in LLC tumor-bearing mice was prevented (Figure 5A). In addition, nilotinib protected against the loss of body weight in LLC-bearing mice (Figure 5B) without affecting tumor volume (Figure 5C). Histology study of LLC tumor in the mice confirmed that nilotinib did not inhibit tumor growth as demonstrated by H&E (Figure S4A) and Ki67 staining (Figure S4B). Further, nilotinib attenuated LLC-induced loss of muscle strength (Figure 5D) as well as loss of TA and extensor digitorum longus (EDL) weight (Figure 5E). Finally, measurement of myofiber cross-sectional area in TA muscle confirmed that nilotinib preserved myofiber mass in LLC tumor-bearing mice (Figure 5F). It is also noteworthy that nilotinib alone did not alter muscle histology (Figure 5F). These data indicate that nilotinib protects against cancer-induced muscle wasting through the suppression of p300 - C/EBPβ signaling.

Nilotinib prolongs survival in KPC tumor-bearing mice

The ultimate goal of managing cancer cachexia is to improve the physical condition of patients and thereby prolong their survival. To determine whether nilotinib treatment can achieve this goal, we conducted a study using the mouse orthotopic KPC tumor model described above due to two considerations. First, the LLC model is generated by subcutaneous implantation of LLC cells and frequently develops skin ulceration, making it infeasible for prolonged study due to animal welfare concerns. Second, the prevalence and severity of cachexia in patients with pancreatic cancer are the highest among all cancer types (4). Consequently, pancreatic cancer has a 5-year survival rate under 10%; and nearly 80% of deaths in patients with advanced pancreatic cancer are associated with severe wasting (31–34). If nilotinib prolongs survival of mice bearing pancreatic cancer, it would be a very strong evidence for its capacity in extending survival for cancer cachexia. As shown in Figure 6A, mice bearing KPC tumor treated with DMSO (vehicle for nilotinib) died between 18 to 28 days after tumor cell implantation (median survival 24.5 days). However, KPC tumor-bearing mice treated with nilotinib survived significantly longer (26 to 34 days; median survival 31 days). Over the course of nilotinib treatment we observed attenuated the loss of muscle function measured as grip strength (Figure 6B), suggesting that the extension of survival by nilotinib treatment is due to the alleviation of muscle wasting. The treatment did not alter tumor volume at the end point (Figure S5). These data demonstrate that the morbidity and mortality of mice bearing pancreatic cancer can be ameliorated by selective inhibition of p38β MAPK using nilotinib, and hence brings forward the possibility of using this drug as an anti-cachexia intervention.

Discussion

The current study identifies p38β MAPK as a necessary and sufficient signaling molecule for the activation of the acetyltransferase activity of p300 towards C/EBPβ through site-specific phosphorylation of p300 on Ser-12 in response to TLR4 activation that causes muscle wasting in cancer host. These data indicate that p38β MAPK orchestrates multiple intricate signaling events that are required for the activation of the muscle protein degradation machinery in response to cancer. This study not only reiterates the key role of p38β MAPK in mediating cancer-induced muscle wasting by reconciling the previous observations that both p300 and p38β MAPK are essential for the development of muscle wasting (11,12), but also demonstrates that selective inhibition of p38β MAPK with nilotinib, an FDA-approved therapy for CML treatment, alleviates muscle wasting in tumor-bearing mice. Thus, the current study has made significant conceptual advances in the underlying etiology of cancer-induced cachexia, and brought about an opportunity for clinical intervention of cancer cachexia by targeting the underlying etiology.

The highly effectiveness of p38β MAPK ablation or inhibition in alleviating cancer-induced muscle wasting is attributed to its central role in the signaling cascade that governs the UPP and ALP machinery (35). Upon activation by TLR4, through p300-mediated acetylation of C/EBPβ on Lys-39 (12) and a direct phosphorylation of C/EBPβ on Thr-188 (9), p38β MAPK activates C/EBPβ to upregulate transcription of the ubiquitin E3 ligases UBR2 and atrogin1/MAFbx as well as the ATG8 family members LC3b and Gabarapl1

(8,10,11). Thereby, C/EBPβ is required for cancer-induced muscle wasting (8). In addition, p38β MAPK directly activates Unc-51 like autophagy activating kinase (ULK1), which is essential for the lipidation process required for autophagosome formation (36), by phosphorylating its Ser-555 residue (11). Due to the regulatory role of p38β MAPK in multiple signaling steps that are rate-limiting for muscle catabolism, it is absolutely required for cancer-induced muscle wasting (11). The current study further demonstrates that p38β MAPK-mediated activation of p300 through phosphorylation of Ser-12 is necessary and sufficient for cancer-induced muscle wasting. Based on these data, we propose a signaling cascade that mediates cancer-induced muscle catabolism through p38β MAPK (Figure 7).

In parallel, cancer induces systemic activation of TLR4 resulting in elevation of circulating cytokines including TNFα and IL-6 (6,7) that promote muscle wasting through at least partially the activation of p38 MAPK (37,38). Other humoral factors that are found in cancer milieu and promote muscle wasting including activin A/myostatin (18,39), TGFβ (40) and TWEAK (41) have been shown to activate p38β MAPK. Moreover, TLR4 may mediate muscle wasting associated with various disorders in response to diverse types of Danger Associated Molecular Patterns (DAMPS) (42). In cancer, TLR4 is activated by circulating Hsp70 and Hsp90 released by cancer cells (7), whereas activation of TLR4 during sepsis and trauma is mediated by lipopolysaccharide (LPS) (21) or high mobility group box-1 (HMGB-1) (43), respectively. As the central mediator of muscle catabolism induced by diverse types of catabolic factors, p38β MAPK could be a therapeutic target of cachexia associated with various pathological conditions.

Due to the lack of an established treatment for cancer cachexia, there is an unmet medical need for a pharmacological solution to this lethal disorder. Our data have demonstrated for the first time that nilotinib is a promising candidate for intervention in cancer-induced cachexia. All kinase inhibitors have relative specificity that is dependent on concentration. Nilotinib was screened for binding affinity to an extensive array of kinases, of which p38β MAPK stood out as one of the a few kinases with highest binding affinity for Nilotinib (Kd = 32 nM) (13). Taking advantage of this rare feature, we demonstrate that Nilotinib completely abrogates p38β MAPK-mediated p300 activation in muscle cells at a very low concentration (500 nM), resulting in preservation of myofibrillar protein myosin heavy chain that is highly susceptible to cancer cachexia. Importantly, nilotinib is 20-fold more potent than the p38α/β MAPK dual inhibitor SB202190 at blocking these effects, and at this concentration nilotinib does not inhibit p38α MAPK-mediated myogenic differentiation, indicating its selectivity for p38β MAPK. It is worth noting that at higher concentrations nilotinib would lose the selectivity for p38β MAPK. In fact, a previous report showed that at 5 μM nilotinib (10 times higher than our effective dose in suppressing myotube atrophy) inhibits C2C12 myoblast differentiation (44). As an FDA-approved drug for CML by inhibiting the BCR-ABL kinase (13), nilotinib was found effective in mouse models of leukemias with therapeutic dose ranging from 15 to 75 mg/kg/day (45,46). Because of its off-target binding with a number of kinases (13), therapeutic doses of nilotinib for leukemia inevitably cause a number of side effects (hcp.novartis.com/tasigna/safety). In contrast, the dose of nilotinib that effectively alleviated muscle wasting in mouse models of cancer cachexia (0.5 mg/kg/day) was at least 30-fold lower than the therapeutic doses for mouse leukemias. Hence, specific inhibition of p38β MAPK and reduction of unwanted

side effects can be achieved. These data suggest that nilotinib can be a safe treatment for cancer cachexia. Given the involvement of p38β MAPK in inflammatory signaling activated by diverse humoral factors discussed above, nilotinib could be effective for intervention in muscle wasting associated with not only cancer but also other pathological conditions. On the other hand, new compounds with even higher specificity for inhibiting p38β MAPK could be developed to combat cancer cachexia.

In summary, we demonstrate in tumor-bearing mice that p38β MAPK is an essential activator for p300 to acetylate C/EBPβ, which is required for the development and progression of muscle wasting in response to TLR4 activation. Importantly, this signaling pathway can be selectively inhibited by utilizing an existing FDA-approved kinase inhibitor, nilotinib, to alleviate muscle wasting and prolong survival. Therefore, future clinical investigations into the efficacy of nilotinib in the therapy of cancer cachexia is warranted.

Supplementary Material

Refer to Web version on PubMed Central for supplementary material.

ACKNOWLEDGEMENT:

This study was supported by an R01 grant from National Institute of Arthritis and Musculoskeletal and Skin Diseases to Y.-P.L. (R01 AR067319) and a grant from National Cancer Institute to Y.-P.L. and M.L. (R01 CA203108).

The authors thank Professor Zanxian Xia of Central South University, China for sharing p300 mutant plasmids (p300-S12A and p300-S89A), Professor Elizabeth Jaffee of Johns Hopkins University for sharing the KPC cells, and Professor Daniel Marks of Oregon Health and Science University for training with orthotopic injection of KPC cells.

References

1. Fearon KC, Glass DJ, Guttridge DC. Cancer cachexia: mediators, signaling, and metabolic pathways. Cell metabolism2012;16:153–66 [PubMed: 22795476]
2. Fearon K, Strasser F, Anker SD, Bosaeus I, Bruera E, Fainsinger RL, et al.Definition and classification of cancer cachexia: an international consensus. Lancet Oncol2011;12:489–95 [PubMed: 21296615]
3. Andreyev HJ, Norman AR, Oates J, Cunningham D. Why do patients with weight loss have a worse outcome when undergoing chemotherapy for gastrointestinal malignancies?Eur J Cancer1998;34:503–9 [PubMed: 9713300]
4. Baracos VE, Martin L, Korc M, Guttridge DC, Fearon KCH. Cancer-associated cachexia. Nat Rev Dis Primers2018;4:17105
5. Siegel RL, Miller KD, Jemal A. Cancer statistics, 2020. CA Cancer J Clin2020;70:7–30 [PubMed: 31912902]
6. Zhang G, Liu Z, Ding H, Miao H, Garcia JM, Li YP. Toll-like receptor 4 mediates Lewis lung carcinoma-induced muscle wasting via coordinate activation of protein degradation pathways. Sci Rep2017;7:2273 [PubMed: 28536426]
7. Zhang G, Liu Z, Ding H, Zhou Y, Doan HA, Sin KWT, et al.Tumor induces muscle wasting in mice through releasing extracellular Hsp70 and Hsp90. Nat Commun2017;8:589 [PubMed: 28928431]
8. Zhang G, Jin B, Li YP. C/EBPbeta mediates tumour-induced ubiquitin ligase atrogin1/MAFbx upregulation and muscle wasting. The EMBO journal2011;30:4323–35 [PubMed: 21847090]
9. Zhang G, Li YP. p38beta MAPK upregulates atrogin1/MAFbx by specific phosphorylation of C/EBPbeta. Skelet Muscle2012;2:20 [PubMed: 23046544]

10. Zhang G, Lin RK, Kwon YT, Li YP. Signaling mechanism of tumor cell-induced up-regulation of E3 ubiquitin ligase UBR2. FASEB journal : official publication of the Federation of American Societies for Experimental Biology2013;27:2893–901 [PubMed: 23568773]
11. Liu Z, Sin KWT, Ding H, Doan HA, Gao S, Miao H, Wei Y, Wang Y, Zhang G, Li Y-P. p38beta MAPK mediates ULK1-dependent induction of autophagy in skeletal muscle of tumor-bearing mice. Cell Stress2018;2:311–24 [PubMed: 31225455]
12. Sin TK, Zhu JZ, Zhang G, Li YP. p300 Mediates Muscle Wasting in Lewis Lung Carcinoma. Cancer Res2019;79:1331–42 [PubMed: 30705122]
13. Manley PW, Drueckes P, Fendrich G, Furet P, Liebetanz J, Martiny-Baron G, et al.Extended kinase profile and properties of the protein kinase inhibitor nilotinib. Biochimica et biophysica acta2010;1804:445–53 [PubMed: 19922818]
14. Foley K, Rucki AA, Xiao Q, Zhou D, Leubner A, Mo G, et al.Semaphorin 3D autocrine signaling mediates the metastatic role of annexin A2 in pancreatic cancer. Sci Signal2015;8:ra77
15. Ma H, Guo M, Shan B, Xia Z. Targeted functional analysis of p300 coactivator in Wnt/beta-catenin signaling pathway using phosphoproteomic and biochemical approaches. J Proteomics2012;75:2601–10 [PubMed: 22465714]
16. Askari N, Beenstock J, Livnah O, Engelberg D. p38 is Active in vitro and in vivo When Monophosphorylated on Thr180. Biochemistry2009;24
17. Hoshino K, Takeuchi O, Kawai T, Sanjo H, Ogawa T, Takeda Y, et al.Cutting edge: Toll-like receptor 4 (TLR4)-deficient mice are hyporesponsive to lipopolysaccharide: evidence for TLR4 as the Lps gene product. J Immunol1999;162:3749–52 [PubMed: 10201887]
18. Ding H, Zhang G, Sin KW, Liu Z, Lin RK, Li M, et al.Activin A induces skeletal muscle catabolism via p38beta mitogen-activated protein kinase. J Cachexia Sarcopenia Muscle2017;8:202–12 [PubMed: 27897407]
19. Michaelis KA, Zhu X, Burfeind KG, Krasnow SM, Levasseur PR, Morgan TK, et al.Establishment and characterization of a novel murine model of pancreatic cancer cachexia. J Cachexia Sarcopenia Muscle2017
20. Hingorani SR, Wang L, Multani AS, Combs C, Deramaudt TB, Hruban RH, et al.Trp53R172H and KrasG12D cooperate to promote chromosomal instability and widely metastatic pancreatic ductal adenocarcinoma in mice. Cancer Cell2005;7:469–83 [PubMed: 15894267]
21. Doyle A, Zhang G, Abdel Fattah EA, Eissa NT, Li YP. Toll-like receptor 4 mediates lipopolysaccharide-induced muscle catabolism via coordinate activation of ubiquitin-proteasome and autophagy-lysosome pathways. FASEB J2011;25:99–110 [PubMed: 20826541]
22. Yang J, Zhang Z, Zhang Y, Ni X, Zhang G, Cui X, et al.ZIP4 Promotes Muscle Wasting and Cachexia in Mice With Orthotopic Pancreatic Tumors by Stimulating RAB27B-Regulated Release of Extracellular Vesicles From Cancer Cells. Gastroenterology2019;156:722–34e6 [PubMed: 30342032]
23. Cuenda A, Rousseau S. p38 MAP-kinases pathway regulation, function and role in human diseases. Biochim Biophys Acta2007;1773:1358–75 [PubMed: 17481747]
24. Perdiguero E, Ruiz-Bonilla V, Gresh L, Hui L, Ballestar E, Sousa-Victor P, et al.Genetic analysis of p38 MAP kinases in myogenesis: fundamental role of p38alpha in abrogating myoblast proliferation. EMBO J2007;26:1245–56 [PubMed: 17304211]
25. Palacios D, Mozzetta C, Consalvi S, Caretti G, Saccone V, Proserpio V, et al.TNF/p38alpha/polycomb signaling to Pax7 locus in satellite cells links inflammation to the epigenetic control of muscle regeneration. Cell Stem Cell2010;7:455–69 [PubMed: 20887952]
26. Ono Y, Sakamoto K. Lipopolysaccharide inhibits myogenic differentiation of C2C12 myoblasts through the Toll-like receptor 4-nuclear factor-kappaB signaling pathway and myoblast-derived tumor necrosis factor-alpha. PLoS One2017;12:e0182040
27. He WA, Berardi E, Cardillo VM, Acharyya S, Aulino P, Thomas-Ahner J, et al.NF-kappaB-mediated Pax7 dysregulation in the muscle microenvironment promotes cancer cachexia. J Clin Invest2013;123:4821–35 [PubMed: 24084740]
28. Sicard P, Clark JE, Jacquet S, Mohammadi S, Arthur JS, O'Keefe SJ, et al.The activation of p38 alpha, and not p38 beta, mitogen-activated protein kinase is required for ischemic preconditioning. Journal of molecular and cellular cardiology2010;48:1324–8 [PubMed: 20188737]

29. O'Keefe SJ, Mudgett JS, Cupo S, Parsons JN, Chartrain NA, Fitzgerald C, et al.Chemical genetics define the roles of p38alpha and p38beta in acute and chronic inflammation. J Biol Chem2007;282:34663–71 [PubMed: 17855341]
30. Lee JK, Hallock PT, Burden SJ. Abelson tyrosine-protein kinase 2 regulates myoblast proliferation and controls muscle fiber length. Elife2017;6
31. Olive KP, Jacobetz MA, Davidson CJ, Gopinathan A, McIntyre D, Honess D, et al.Inhibition of Hedgehog signaling enhances delivery of chemotherapy in a mouse model of pancreatic cancer. Science2009;324:1457–61 [PubMed: 19460966]
32. Palesty JA, Dudrick SJ. What we have learned about cachexia in gastrointestinal cancer. Dig Dis2003;21:198–213 [PubMed: 14571093]
33. Martignoni ME, Kunze P, Friess H. Cancer cachexia. Mol Cancer2003;2:36 [PubMed: 14613583]
34. Wesseltoft-Rao N, Hjermstad MJ, Ikdahl T, Dajani O, Ulven SM, Iversen PO, et al.Comparing two classifications of cancer cachexia and their association with survival in patients with unresected pancreatic cancer. Nutr Cancer2015;67:472–80 [PubMed: 25710201]
35. Sin TK, Zhang G, Zhang Z, Gao S, Li M, Li YP. Cancer Takes a Toll on Skeletal Muscle by Releasing Heat Shock Proteins-An Emerging Mechanism of Cancer-Induced Cachexia. Cancers (Basel)2019;11
36. Lin MG, Hurley JH. Structure and function of the ULK1 complex in autophagy. Curr Opin Cell Biol2016;39:61–8 [PubMed: 26921696]
37. Li YP, Chen Y, John J, Moylan J, Jin B, Mann DL, et al.TNF-alpha acts via p38 MAPK to stimulate expression of the ubiquitin ligase atrogin1/MAFbx in skeletal muscle. FASEB J2005;19:362–70 [PubMed: 15746179]
38. Puppa MJ, Gao S, Narsale AA, Carson JA. Skeletal muscle glycoprotein 130's role in Lewis lung carcinoma-induced cachexia. FASEB journal : official publication of the Federation of American Societies for Experimental Biology2014;28:998–1009 [PubMed: 24145720]
39. Zhong X, Pons M, Poirier C, Jiang Y, Liu J, Sandusky GE, et al.The systemic activin response to pancreatic cancer: implications for effective cancer cachexia therapy. J Cachexia Sarcopenia Muscle2019;10:1083–101 [PubMed: 31286691]
40. Greco SH, Tomkotter L, Vahle AK, Rokosh R, Avanzi A, Mahmood SK, et al.TGF-beta Blockade Reduces Mortality and Metabolic Changes in a Validated Murine Model of Pancreatic Cancer Cachexia. PLoS One2015;10:e0132786
41. Kumar A, Bhatnagar S, Paul PK. TWEAK and TRAF6 regulate skeletal muscle atrophy. Curr Opin Clin Nutr Metab Care2012;15:233–9 [PubMed: 22366923]
42. Erridge C. Endogenous ligands of TLR2 and TLR4: agonists or assistants?Journal of leukocyte biology2010;87:989–99 [PubMed: 20179153]
43. Yang H, Wang H, Chavan SS, Andersson U. High Mobility Group Box Protein 1 (HMGB1): The Prototypical Endogenous Danger Molecule. Mol Med2015;21 Suppl 1:S6–S12 [PubMed: 26605648]
44. Contreras O, Villarreal M, Brandan E. Nilotinib impairs skeletal myogenesis by increasing myoblast proliferation. Skelet Muscle2018;8:5 [PubMed: 29463296]
45. Kaur P, Feldhahn N, Zhang B, Trageser D, Muschen M, Pertz V, et al.Nilotinib treatment in mouse models of P190 Bcr/Abl lymphoblastic leukemia. Mol Cancer2007;6:67 [PubMed: 17958915]
46. Weisberg E, Catley L, Wright RD, Moreno D, Banerji L, Ray A, et al.Beneficial effects of combining nilotinib and imatinib in preclinical models of BCR-ABL+ leukemias. Blood2007;109:2112–20 [PubMed: 17068153]

Significance:

Findings demonstrate that prevention of p38β MAPK-mediated activation of p300 by the FDA-approved kinase inhibitor nilotinib ameliorates cancer cachexia, representing a potential therapeutic strategy against this syndrome.

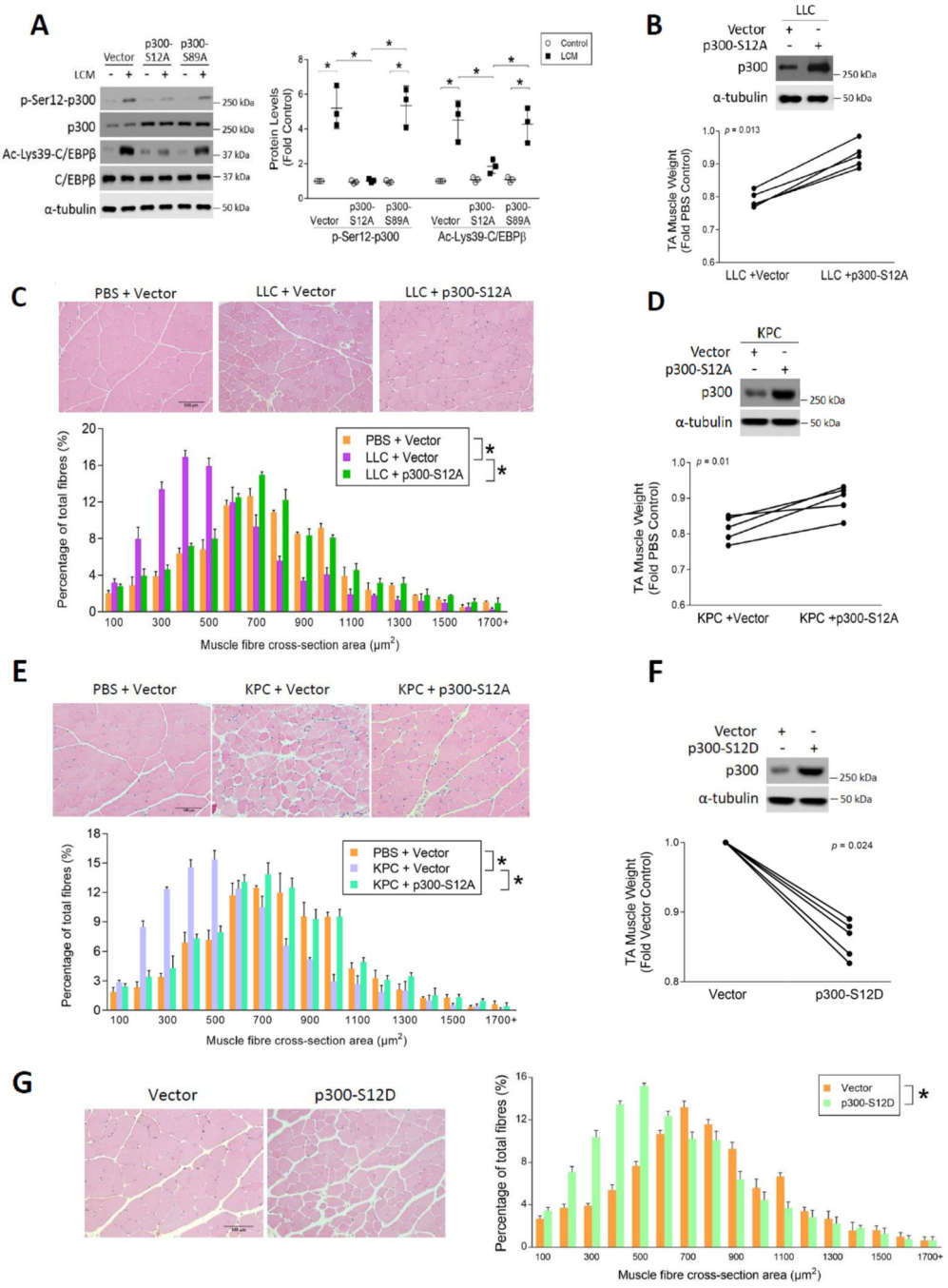

Figure 1. Site-specific phosphorylation of 300 on Ser-12 induced by LLC is necessary and sufficient for the activation C/EBPβ and muscle wasting.

(A) LLC induces p300 phosphorylation on Ser-12 and this reaction is critical to p300-mediated acetylation and activation of C/EBPβ. C2C12 myoblasts were transfected with a plasmid encoding phosphorylation-defective mutant of p300, p300-S12A or p300-S89A, or empty vector as control in 3 independent experiments. After differentiation, myotubes were treated with LLC cell conditioned medium (LCM) or conditioned medium of non-tumorigenic NL20 cells for 2 h. Cell lysates were analyzed by Western blotting. **(B)**

Overexpression of p300-S12A attenuates muscle weight loss in LLC tumor-bearing mice. Tibialis muscle (TA) of LLC tumor-bearing mice was transfected with the p300-S12A-encoding plasmid (n = 5). The contralateral TA was transfected with empty vector as control. After the development of cachexia, TA muscles were collected and weighed on day 21. Overexpression of p300-S12A was confirmed by Western blotting analysis against p300. **(C)** Overexpression of p300-S12A prevents the loss of myofiber mass in LLC tumor-bearing mice. H&E-stained TA cross sections of (B) were analyzed for myofiber cross-sectional area. **(D)** Overexpression of p300-S12A in TA attenuates muscle weight loss in KPC tumor-bearing mice (n = 5). **(E)** Overexpression of p300-S12A in TA prevents the loss of myofiber mass of KPC tumor-bearing mice (n = 5). **(F)** Overexpression of p300-S12D in TA causes loss of muscle weight in cancer-free mice (n = 5). **(G)** Overexpression of p300-S12D in TA causes loss of myofiber mass in cancer-free mice (n = 5). * indicates a statistically significant difference ($p < 0.05$) determined by one-way ANOVA (A), paired Student t-test (B, D and F) or Chi-square test (C, E and G).

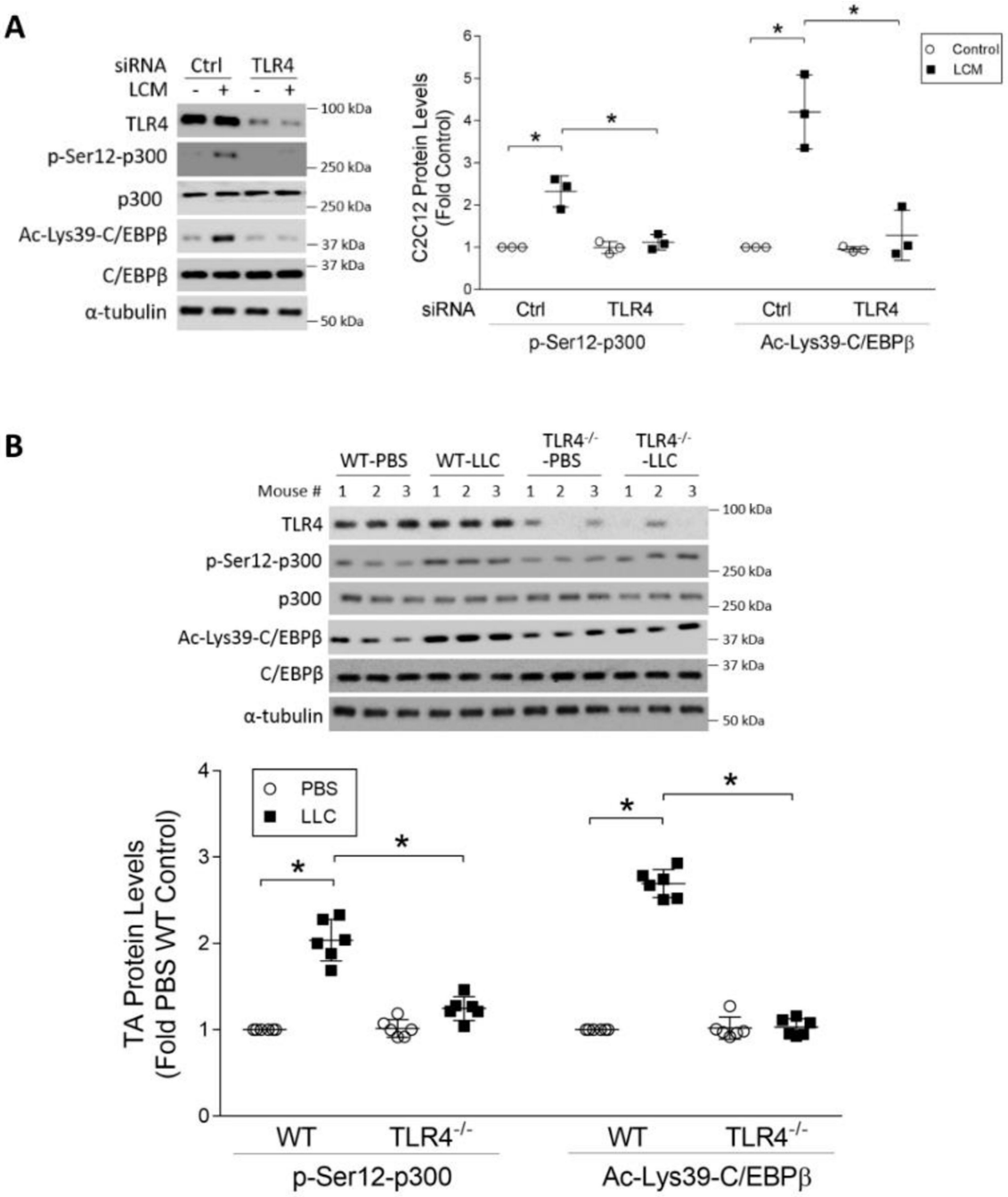

Figure 2. TLR4 mediates LLC-induced p300 phosphorylation on Ser-12.

(A) TLR4 is critical to p300 phosphorylation on Ser-12 and C/EBPβ acetylation on Lys-39 in LCM-treated myotubes. C2C12 myoblasts were transfected with siRNA specific for TLR4 or scrambled control siRNA (n = 3). Differentiated myotubes were treated with LCM for 2 h. Cell lysates were analyzed by Western blotting. **(B)** TLR4 is required for p300 phosphorylation on Ser-12 and C/EBPβ acetylation on Lys-39 in the muscle of LLC tumor-bearing mice. Wild type (WT) and TLR4$^{-/-}$ mice were implanted with LLC cells or injected with PBS as control (n = 6). In 21 days TA muscle were analyzed by Western

blotting. * indicates a statistically significant difference ($p < 0.05$) determined by one-way ANOVA.

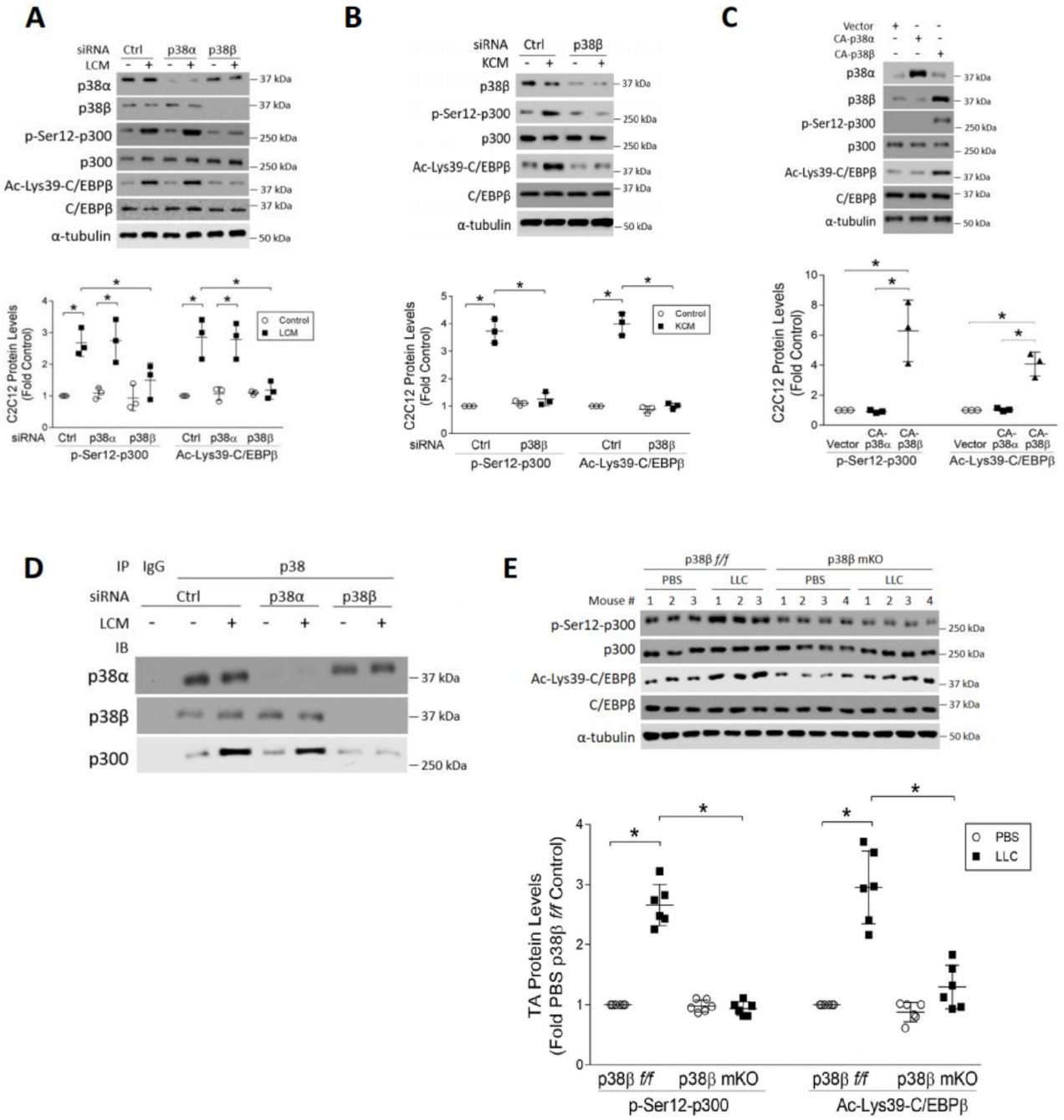

Figure 3. Multiple types of cancer induce p300 phosphorylation on Ser-12 through p38β MAPK.

(A) LCM-induced Ser-12 phosphorylation of p300 in myotubes requires p38β MAPK. C2C12 myoblasts were transfected with siRNA specific for p38α MAPK or p38β MAPK, or scrambled control (n = 3). Differentiated myotubes were treated with LCM for 2 h, the cell lysates were analyzed by western blotting as indicated. **(B)** KCM induces Ser-12 phosphorylation of p300 in myotubes in a p38β MAPK-dependent manner. C2C12 myotubes transfected with p38β MAPK-specific or scrambled siRNA were treated with KCM for 2 h. The cell lysates were analyzed by western blotting as indicated (n = 3). **(C)**

Overexpression of constitutively active p38β MAPK is sufficient to phosphorylate Ser-12 of p300. C2C12 myoblasts were transfected with a plasmid encoding either a constitutively active mutant of p38α MAPK or p38β MAPK. Differentiated myotubes were analyzed by Western blotting as indicated (n = 3). **(D)** LCM stimulates an interaction between p300 and p38β MAPK, but not p38α MAPK. C2C12 myotubes were transfected with either p38α or p38β MAPK-specific siRNAs, and then treated with LCM for 2 h. Immunoprecipitation of p38 MAPK from the cell lysates was performed with pre-immune IgG as a control. Precipitates were then analyzed by Western blotting to verify the knockdown effects and coprecipitation of p300. **(E)** Activation of p300 in the TA muscle of LLC tumor-bearing mice requires p38β MAPK. LLC cells were implanted to p38β MAPK muscle-specific knockout mice (p38β mKO) and p38β MAPK-floxed mice ($p38\beta^{f/f}$) (n = 6). In 21 days mice were euthanized and TA lysates were analyzed by Western blotting as indicated. * signifies a statistically significant difference ($p < 0.05$) determined by one-way ANOVA.

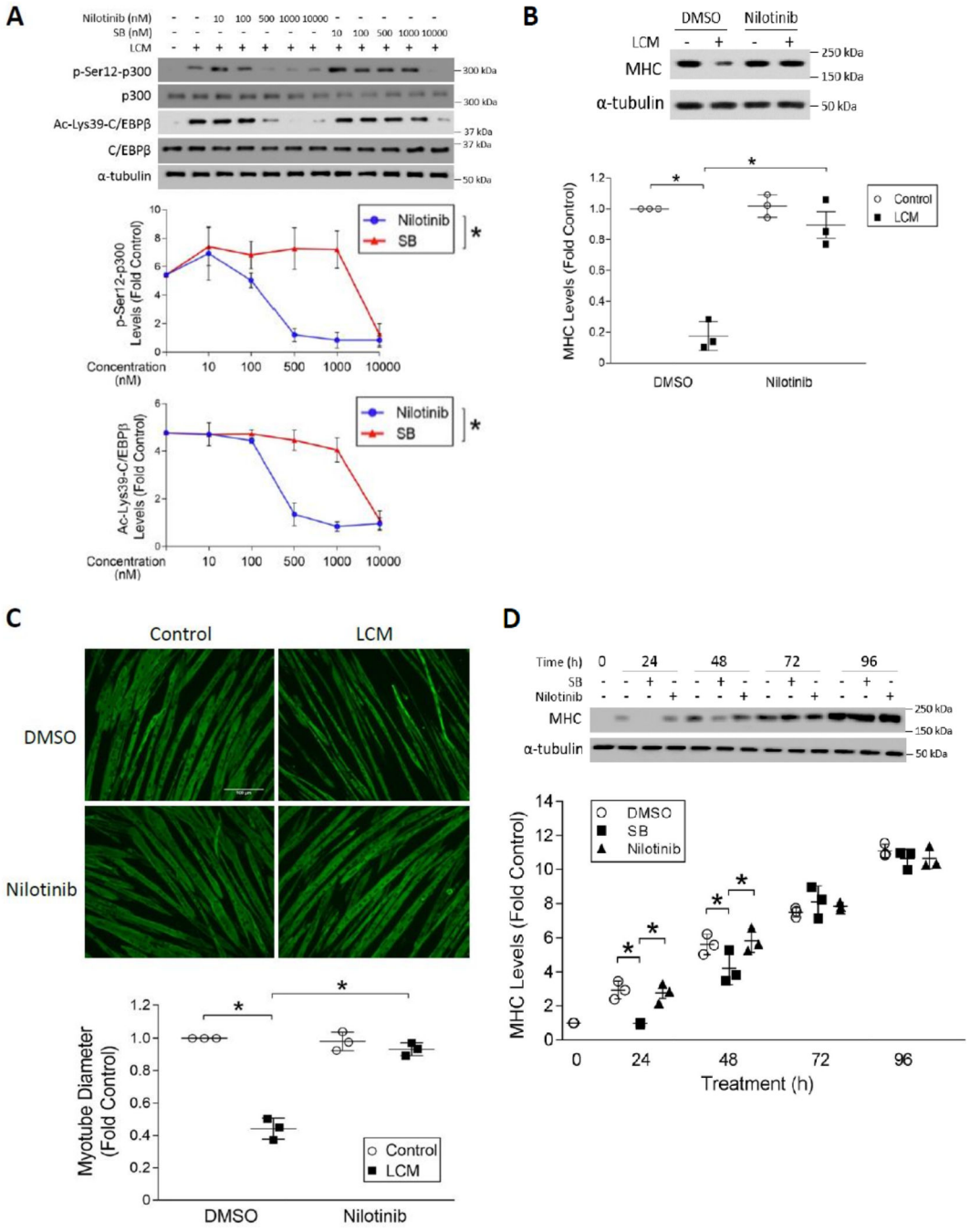

Figure 4. Selective inhibition of p38β MAPK by nilotinib abrogates LLC-induced myotube catabolism without inhibiting myogenesis.

(A) Nilotinib is ~20-fold more potent than SB202190 in the inhibition of LLC-induced activation of p300. C2C12 myotubes were pre-treated with either nilotinib or SB202190 (SB) at indicated doses for 30 mins followed by 2 h of LCM treatment (n = 3). Activation of p300 and C/EBPβ were analyzed by Western blotting as indicated. **(B)** Nilotinib abrogates LCM-induced loss of MHC in myotubes. Myotubes pre-treated with 500 nM of nilotinib or DMSO were incubated with LCM for 72 hrs. Cell lysates were analyzed

for MHC levels by Western blotting (n = 3). **(C)** Nilotinib abolishes LLC-induced loss of myotube mass. Myotubes treated as described in (B) were subjected to immunofluorescence staining of MHC. Diameter of myotubes was measured. **(D)** Nilotinib does not suppress myoblast differentiation at the dose that antagonizes LLC-induced myotube atrophy. C2C12 myoblasts were cultured with differentiation medium containing 10 μM SB202190 (SB), 500 nM nilotinib or DMSO for the indicated time periods. MHC content in the cell lysates were analyzed by Western blotting at indicated times (n = 3). * signifies a statistically significant difference ($p < 0.05$) determined by one-way ANOVA.

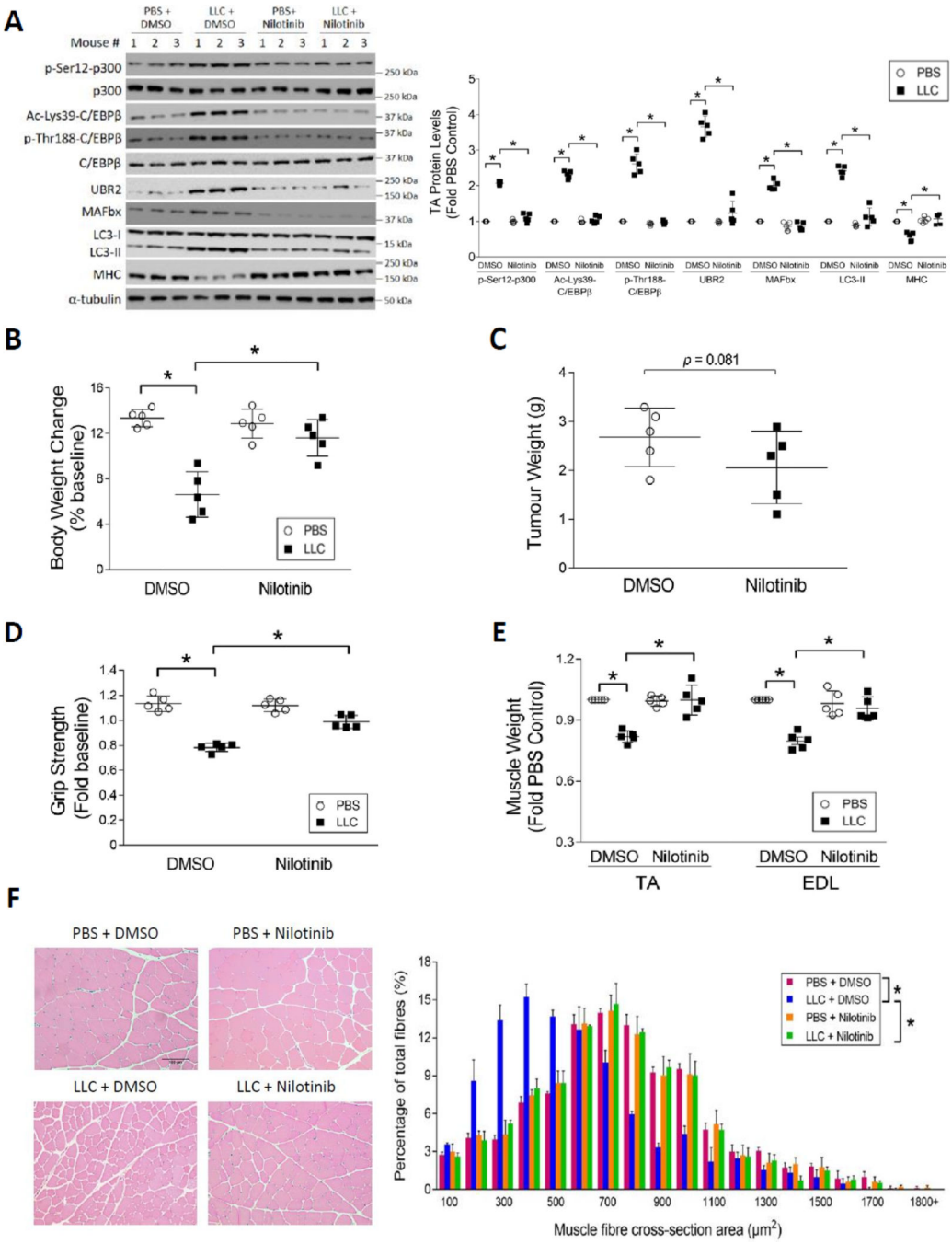

Figure 5. Nilotinib ameliorates muscle wasting by attenuating the catabolic response in LLC tumor-bearing mice.

Nilotinib (0.5 mg/kg/day) or DMSO was administered intraperitoneally to mice 7 days after LLC cell implantation for 14 days. Mice were euthanized on day 21. The tumor was isolated and weighed, and then the net body weight was measured. Muscle samples were collected immediately for analyses of muscle wasting (n = 5). **(A)** Nilotinib abrogates p300 activation and catabolic response in LLC tumor-bearing mice. Catabolic markers in TA muscle lysates were analyzed by Western blotting. **(B)** Nilotinib prevents body weight loss in LLC-bearing

mice. **(C)** Nilotinib does not affect LLC tumor growth. **(D)** Nilotinib preserves skeletal muscle function in LLC tumor-bearing mice. Grip strength was measured on the day of euthanasia. **(E)** Nilotinib attenuates skeletal muscle weight loss in LLC tumor-bearing mice. **(F)** Nilotinib protects against the loss of myofiber mass in LLC tumor-bearing mice. H&E-stained TA cross sections were analyzed for the myofiber cross-sectional area. * signifies a statistically significant difference ($p < 0.05$) determined by one-way ANOVA (A-E) or Chi-square test (F).

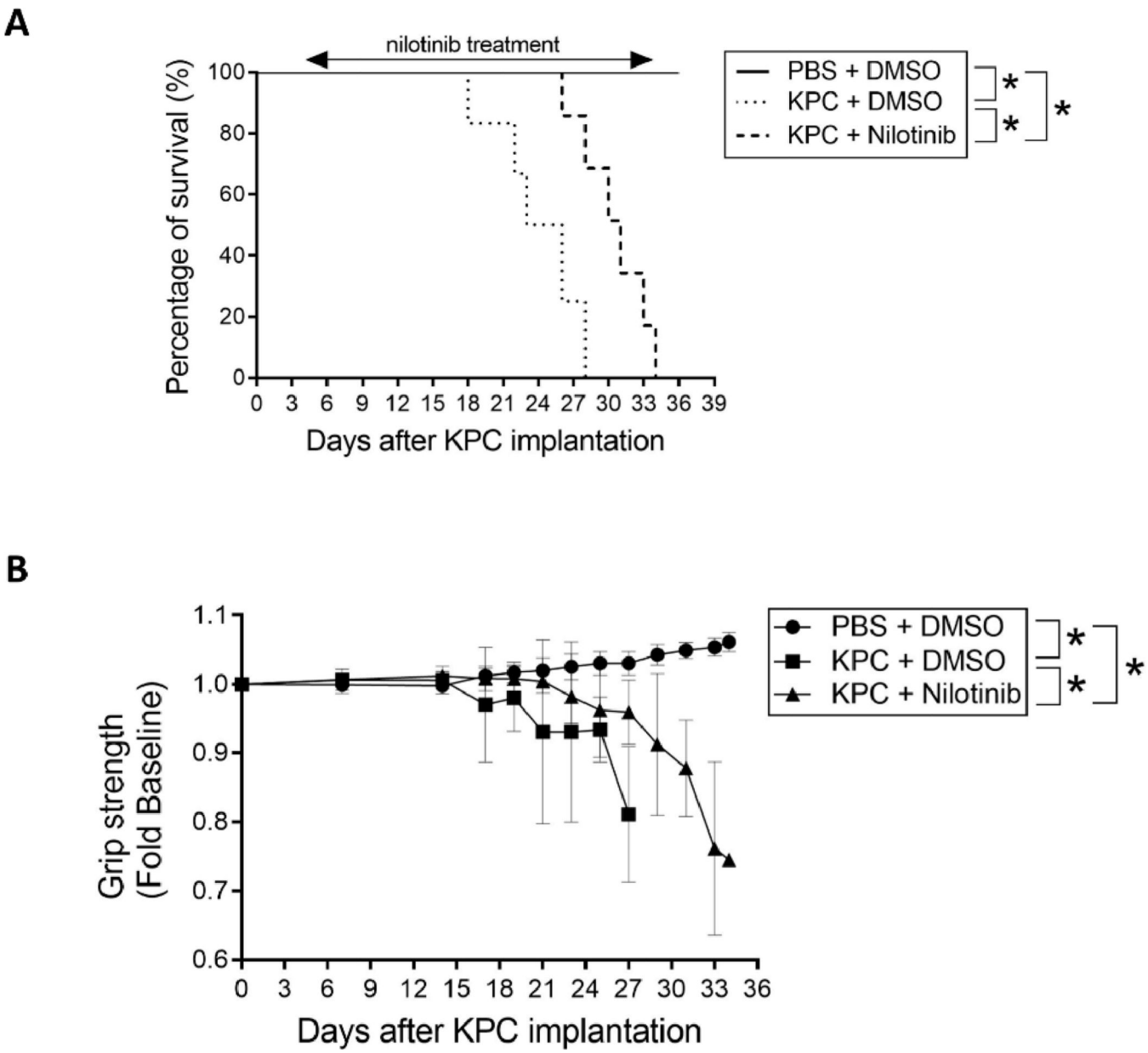

Figure 6. Nilotinib prolongs survival of mice bearing pancreatic cancer by impeding the development of muscle wasting.

Five days after orthotopic implantation of KPC cells to mice, nilotinib (0.5 mg/kg/day) or DMSO were administered intraperitoneally until all tumor-bearing mice reached predetermined end point (n = 7). **(A)** Nilotinib prolongs survival of mice bearing KPC tumor. Survival of KPC tumor-bearing mice was recorded and analyzed using the Kaplan–Meier survival curve. **(B)** Nilotinib impedes the loss of muscle strength in mice bearing KPC tumor. Forelimb grip strength of the mice was monitored over the course of the survival study. Data were analyzed by 2-way ANOVA. * signifies a statistically significant difference ($p < 0.05$).

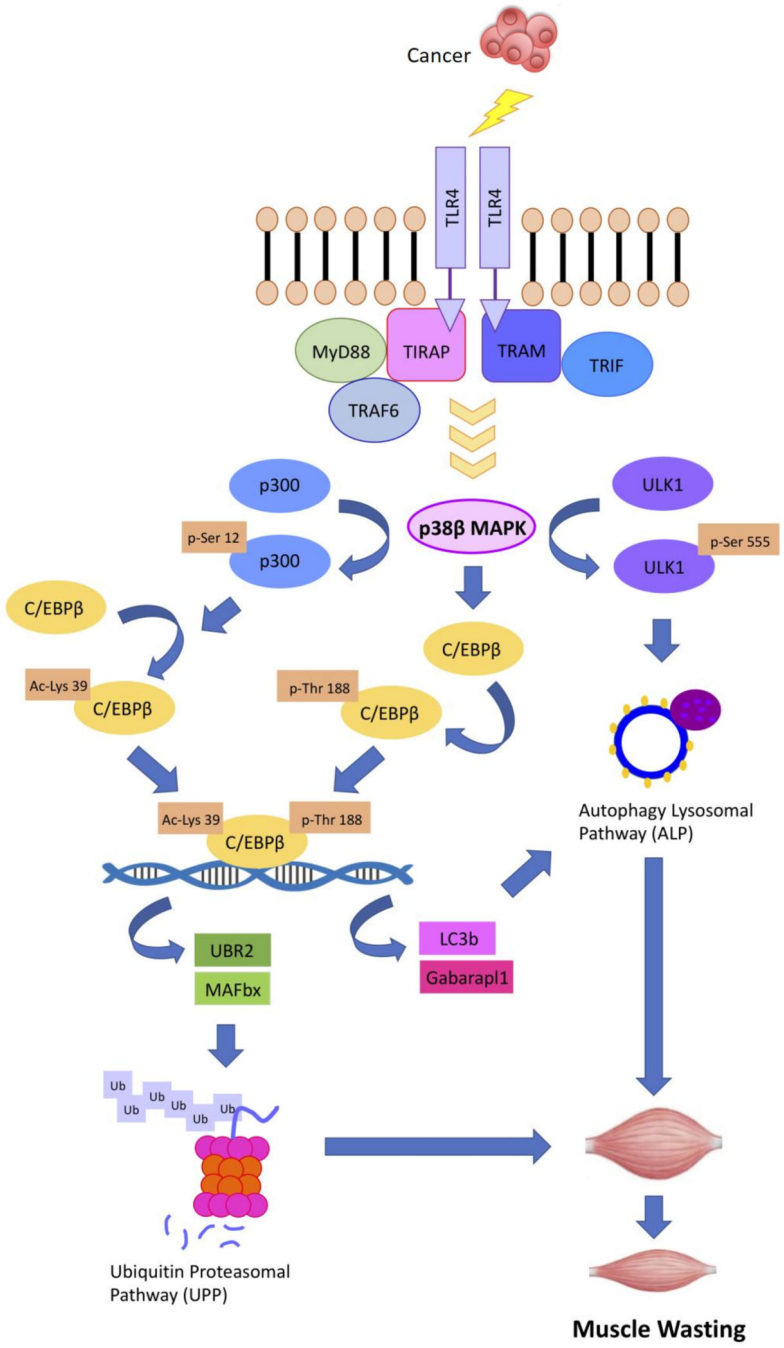

Figure 7.

A graphic illustration of the central role of p38β MAKP in mediating muscle catabolism in response to TLR4 activation based on data from the current and previous studies.